Line tying of interchange modes in a nearly collisionless mirror-trapped plasma

Guy Vandegrift
Department of Physics and Astronomy, Dickinson College, Carlisle, Pennsylvania 17013

(Received 10 February 1989; accepted 15 August 1989)

If the confining potential of electrostatically trapped electrons fluctuates, then the number of trapped electrons also fluctuates. The linear relationship between potential fluctuations and the number of trapped electrons is investigated, considering two loss mechanisms for a nearly collisionless plasma: (1) small-angle collisions (diffusion), and (2) large-angle collisions. This nearly collisionless model predicts the line tying of interchange modes in a mirror-trapped plasma is orders of magnitude larger than previously thought for a fusion plasma, yet still not strong enough to completely line tie an axisymmetric mirror. Also, a nonlinearity in the response can occur at low amplitude.

I. INTRODUCTION

The following problem arises from the study of interchange modes in a magnetic mirror-trapped plasma. A steady source injects electrons into a potential well. Each electron is confined for many bounces until it gains enough energy from collisions to escape. Let the height of the potential well make small fluctuations. How does the number of trapped electrons fluctuate?

It has been proposed to suppress interchange modes in an axisymmetric mirror[1-5] using the interaction of the plasma with the end wall, which is where the magnetic field lines terminate. This process, called "line tying," can be enhanced using feedback stabilization,[6] or blanket stabilization,[2-5] which is the stabilization of a hot plasma by an annular blanket of cold, line-tied plasma. It is useful to focus on a single tube of magnetic flux moving perpendicular to the magnetic field according to the $\mathbf{E}\times\mathbf{B}$ drift. The fluctuating electrostatic potential remains constant along a magnetic field line in the presence of interchange modes.[7-10] The interchange mode introduces charge into the flux tube via higher-order drifts such as the curvature drift and ion polarization drift. Since the interchange mode causes the potential well to fluctuate, a fluctuating current of electrons will leave the flux tube axially, hitting the end wall. This can influence the dynamics of the interchange mode. We shall refer to the relation between fluctuating potential and electron density as the *response* $R(\omega)$.

Electrons in a magnetic mirror are confined by a combination of a magnetic mirror and an electrostatic potential that maintains plasma neutrality by setting the electron loss rate equal to the ion loss rate. We neglect radial losses, as well as fluctuations in the loss rate of ions. For a simple mirror without electron emitting end walls, the electrostatic potential is believed to decrease monotonically from the end wall to the plasma.[1,11,12]

A model to describe the response was proposed by Kunkel and Guillory,[1] and later modified by several authors.[5,6,9,10,13] The "Kunkel–Guillory" model assumes that the electron velocity distribution obeys the Maxwell–Boltzmann distribution, even near the loss boundary. This can occur if the electron mean-free path is short compared to the length of the mirror. Kunkel and Guillory proposed the existence of a cold plasma located near the end wall that might cause the required collisionality, but it would be necessary to prevent the electrons in the cold plasma from interacting with the mirror-trapped plasma.

Volosov and Bekhtenev[14,15] proposed a collisionless response, valid when the mean-free path for electrons is much longer than the length of the device. They assumed that electrons are scattered by small-angle Coulomb collisions. The purpose of this paper is to extend the model by Volosov and Bekhtenev to include large-angle collisions and to compare predictions of the various models for different plasma regimes. We also investigate conditions that modify the response: A nonlinearity can occur at low amplitude, and the response can be very sensitive to turbulence near the end wall.

There are three reasons for looking at the response in the presence of large-angle collisions. First, we must determine desired plasma and vacuum parameters for a magnetic mirror at Dickinson College.[16] A small plasma device often has considerable background gas that can cause large-angle collisions. Second, typically 10% of collisions in a fully ionized plasma are large angle,[17,18] so one should verify that the response due to these large-angle collisions does not overwhelm the response due to small-angle collisions (this is verified). Finally, this response could be of interest in other areas of plasma physics, since electrons are often confined by potential barriers. The ideas presented here can apply the electrons in an unmagnetized plasma, to all-electron plasmas, and perhaps even to electrons in a semiconductor device.

In Sec. II, a simple one-dimensional model is presented that considers both large-angle and small-angle collisions. Although the assumptions are unrealistic, this model yields exact solutions. It also points out an important nonlinearity that occurs at high frequency, and it will help us understand the full three-dimensional model described in Sec. III. Application to interchange modes is discussed in Sec. IV, where we conclude that line tying in a fusion reactor is orders of magnitude greater than previously thought.

 0899-8221/89/122414-08$01.90

II. ONE-DIMENSIONAL MODEL

Consider a one-dimensional square well potential with a depth $\phi_0 = \frac{1}{2}v_0^2$, so that any electron with velocity greater than v_0 will escape. Electrons are placed in the well with zero velocity and gain energy via collisions until v exceeds v_0, whereby the electron exits. Let ν_L be the rate at which electrons encounter large-angle collisions, and ν_s be the inverse time for an electron to random walk via small-angle collisions by an amount $2^{1/2}v_0$ in velocity space. The potential fluctuates as the real part of $\phi = \phi_0 = \phi_1 \exp(i\omega t)$, where $\phi_1 \ll \phi_0$. The number of trapped electrons is $n_0 + n_1 \exp(i\omega t)$, and the response R is defined as

$$n_1/n_0 = R(\omega)(\phi_1/\phi_0). \tag{1}$$

The time ν_{Te}^{-1} for electrons to transit the potential well of length l is assumed much smaller than any of the other frequencies: $\nu_{Te} = v_0/l \gg (\omega, \nu_L, \nu_s)$. In this section we assume that the bounce-averaged velocity space distribution $f(v,t)$ obeys a simple diffusion equation with a source S at $v = 0$, plus two terms representing large angle collisions,

$$\frac{\partial f}{\partial t} = D\frac{\partial^2 f}{\partial v^2} - \nu_L f + \nu_L \frac{n}{2\nu_A} + S\delta(v), \tag{2}$$

with the boundary condition that $f(v,t)$ vanish at the "loss boundary" $v^2/2 = \phi(t) = \phi_0 + \phi_1$. The term containing $n = \int f(v)dv$ in Eq. (2) represents electrons scattered into a point in velocity space after a large-angle collision elsewhere. An electron has probability $b = v_0/v_A < 1$ of remaining trapped after each large-angle collision. The diffusion coefficient D is related to the small-angle scattering frequency ν_s as follows. Define

$$\begin{aligned} \nu_s &= D/v_0^2, \\ \alpha^2 &= \nu_L/\nu_s, \\ b &= v_0/v_A, \\ \beta^2 &= (\nu_L + i\omega)/\nu_s. \end{aligned} \tag{3}$$

Equation (2) can be separated into equilibrium and time-varying parts. Equations for both f_0 and $f_1 e^{i\omega t}$ obey Eq. (2) except that $\partial f_0/\partial t$ is absent from the unperturbed equation, and the equation for f_1 does not contain the source term $S\delta(v)$. The solutions to the unperturbed and perturbed parts of Eq. (2) are

$$F_0(x) = \frac{b}{2} - \frac{b}{2}\cosh(\alpha - \alpha x) + \frac{1}{2}\frac{b\sinh\alpha + (1-b)\alpha}{\cosh\alpha - 1}\sinh(\alpha - \alpha x), \tag{4a}$$

$$F_1(x) = \left[\frac{b\alpha^2}{2\beta^2} + \frac{\beta}{2}\left(1 - \frac{b\alpha^2}{2\beta^2}\right)\frac{\cosh(\beta x)}{\sinh\beta}\right]N_1, \tag{4b}$$

where $F = v_0 f/n_0$, $N = n/n_0$, and $x = v/v_0$. Figure 1 shows $f_0(v)$ for different relative strengths α of small- and large-angle collisions.

The solution (4b) for the perturbed distribution function contains a constant $n_1 = \int f_1\, dv$, which can be found using the boundary condition that $f_0 + f_1$ must vanish at the "loss boundary": $f(v_0 + v_1) = 0$, where $2v_1/v_0 = \phi_1/\phi_0$ represents the shift in the loss boundary due to the perturbation. We approximate $f_0(v_0 + v_1)$ as $f_0(v_0) + v_1\, \partial f_0/\partial v$, and $f_1(v_0 + v_1)$ as $f_1(v_0)$. Using $f_0(v_0) = 0$ we obtain the boundary condition

$$f_1(v_0) = -v_1\frac{\partial f_0(v_0)}{\partial v} \tag{5}$$

and the response

$$R(\omega) = \frac{\frac{1}{2}[b\alpha\sinh\beta + (1-b)\alpha^2]/(\cosh\alpha - 1)}{b\alpha^2/\beta^2 + (1 - \alpha^2/\beta^2)\beta\coth\beta}. \tag{6}$$

Figures 2 and 3 show $|R(\omega)|$ for real and imaginary ω. The poles of $R(\omega)$ along the imaginary axis are physical, corresponding to a decay of density to the equilibrium value at constant potential. These poles are probably unimportant for line tying because they represent exponentially decaying modes, while plasma stability issues involve exponentially growing modes.

The inverse confinement time ν_c is the rate at which particles leave the unperturbed well: $\nu_c n = \partial n/\partial t$. To calculate ν_c, we integrate Eq. (2) over the delta function at $v = 0$. Or, we can add the loss rate due to collisions to the loss rate due to diffusion at $v = \pm v_0$:

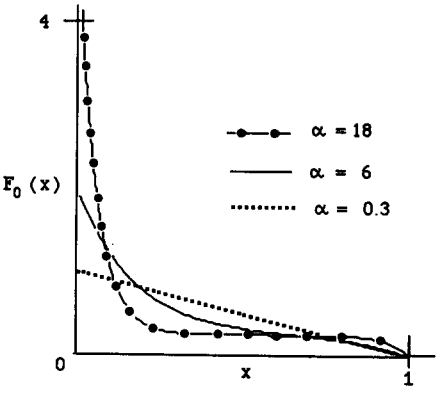

FIG. 1. Equilibrium distribution functions $f_0(v)$ in the one-dimensional model for $b = 0.5$. The three curves represent dominance by small-angle scattering ($\alpha = 0.3$), transition ($\alpha = 6$), and dominance by large-angle collisions ($\alpha = 18$). Note that when large-angle collisions dominate ($\alpha \gg 1$), f_0 peaks sharply at the source ($v = 0$), falls to a plateau region f^*, then drops sharply to zero at the loss boundary $x = v/v_0 = 1$.

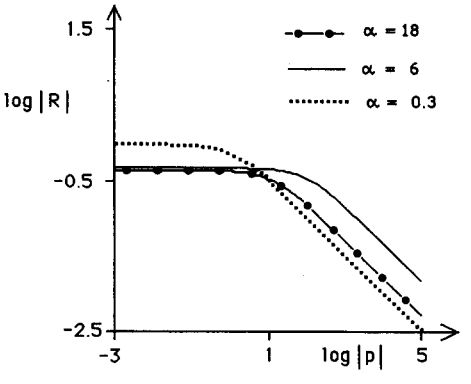

FIG. 2. Linear response for p real, where $p = i\omega/\nu_s$. This corresponds to an exponentially growing model. Three values of α are $\alpha = 0.3$, 6, and 18.

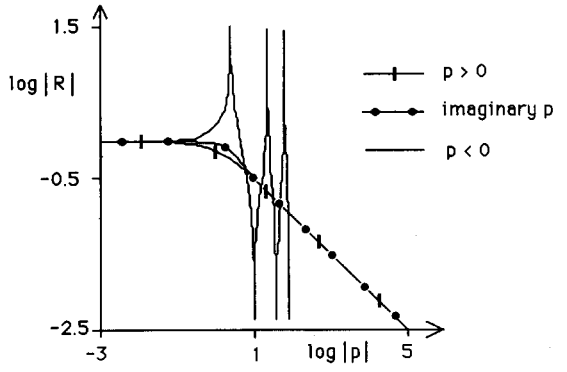

FIG. 3. Comparison of the response for $p = i\omega/\nu_s > 0$ (exponential growth), $p < 0$ (exponential decay), and $p = i\omega/\nu_s$ imaginary (oscillating wave). Parameters are $b = 0.5$ and $\alpha = 6$. The poles and zeros of R occur for an exponentially decaying signal $p = i\omega/\nu_s < 0$.

$$\nu_c n_0 = -2D\frac{\partial f_0(0)}{\partial v} \tag{7a}$$

$$= -2D\frac{\partial f_0(v_0)}{\partial v} + (1-b)\nu_L n_0. \tag{7b}$$

Both methods yield the same result:

$$\nu_c = \frac{b\alpha \sinh\alpha + (1-b)\alpha^2\cosh\alpha}{\cosh\alpha - 1}\nu_s. \tag{8}$$

The inverse confinement time ν_c and response $R(\omega)$ for various limits involving ν_c, ν_s, ν_L, and ω are shown in Table I. The results can be approximately summarized as

$$R(\omega) \sim 1, \quad \text{if } \omega \ll \nu_c, \tag{9a}$$

$$R(\omega) \sim \sqrt{\nu_c/i\omega}, \quad \text{if } \omega \gg \nu_c, \tag{9b}$$

where one takes the branch of $(i\omega)^{-1/2}$ with a positive real part. The ambiguity when the real part of $(i\omega)^{-1/2}$ vanishes is resolved by putting a branch line from $\omega = 0$ to infinity along the positive imaginary axis, so that Eq. (9b) does not describe pure exponentially decaying signals. With this sign convention, we may interpret n as the number of trapped electrons, and ϕ as the electrostatic potential of the flux tube, with the end wall potential held constant.

Equation (9a) is a simplified version of the response obtained in Ref. 15. However, at very low frequency $\omega \ll \nu_s$ or $\ll \nu_L$, Eq. (9b) disagrees with Eq. (18) of Ref. 15. At very low frequency, the response [Eq. (6)] can be shown to be equivalent to the obvious equation $n_1/\phi_1 = \delta n_0/\delta\phi_0$, where the derivative is taken at constant source. The low-frequency response in Ref. 15 was obtained by taking the derivative of the axial loss of electrons $j = \partial n/\partial t: j_1/\phi_1 = \delta j_0/\delta\phi_0$ at constant density, where $j_1 = i\omega n_1$. We argue that (9b) of this paper is the correct low-frequency response as follows. When $\omega < \nu_c$ it is necessary to assume that a source maintains the unperturbed parameters at constant values in order to postulate linear waves with time dependence $\exp(i\omega t)$, so that a perturbation in potential leads not to a perturbation in exiting current (which equals the source at low frequency), but to a perturbation in the total number of trapped electrons.

TABLE I. The simple one-dimensional model yields approximations for the response $R(\omega)$ and the equilibrium confinement time ν_c^{-1} in various limits involving the relative magnitudes of large-angle collision frequency ν_L, small-angle collision frequency ν_s, and mode frequency ω.

	Small-angle collisions dominate	Large-angle collisions dominate
High-frequency fluctuations	$R = \sqrt{\nu_s/i\omega}$ $\omega \gg \nu_s \gg \nu_L$	$R = (b/2)\sqrt{\nu_L/i\omega}$ $\omega \gg \omega_L \gg \nu_s$
Low-frequency fluctuations	$R = 1$ $\nu_s \gg \omega \gg \nu_L$ $\nu_s \gg \nu_L \gg \omega$	$R = \frac{1}{2}b/(1-b)$ $\nu_L \gg \omega \gg \nu_s$ $\nu_L \gg \nu_s \gg \omega$
Equilibrium inverse confinement time	$\nu_c = 2\nu_s$ $\nu_s \gg \nu_L$	$\nu_c = (1-b)\nu_L$ $\nu_L \gg \nu_s$

It is interesting to compare the collisionless response with collisional response (proposed by Kunkel and Guillory[1]), which is valid if the mean-free path for collisions is shorter than the length of the system:

$$R_{KG}(\omega) \sim \nu_c/i\omega. \tag{10}$$

The interchange mode typically has a frequency near the ion transit frequency: $\omega \sim \nu_{Ti}$. Since ν_{Ti}/ν_c is the number of bounces a typical ion makes before escaping the mirror, we see that the new response is much larger than the Kunkel–Guillory response whenever ions are confined for many bounces. Line tying in a nearly collisionless plasma can be orders of magnitude stronger than the Kunkel–Guillory model would have predicted.

An important nonlinearity may occur at high frequency even if $\phi_1 \ll \phi_0$. In the limit $\omega \gg \nu_c$, the perturbed distribution function ϕ_1 can be obtained from Eq. (4b) in the region near the loss boundary $v = v_0$:

$$f_1(v) = \left[\frac{1}{2v_0}\sqrt{\frac{i\omega}{\nu_s}}\exp\left(-\sqrt{\frac{i\omega}{\nu_s}}\frac{\Delta v}{v_0}\right)\right] n_1, \tag{11}$$

where $\Delta v = v_0 - v$ is the distance in from the unperturbed loss boundary. Thus, at high frequency, $f_1(v)$ is concentrated very close to the loss boundary, decaying with a skin depth of $v_0(\nu_s/\omega)^{1/2}$ as one moves away from the loss boundary. However, in obtaining the linear response, we assumed in Eq. (5) that $f_1(v)$ did not vary too rapidly, so that $f_1(v_0) \approx f_1(v_0 + v_1)$. Consequently, to be in the linear regime at high frequency we require

$$\phi_1/\phi_0 \ll \sqrt{\nu_s/\omega} \ll 1. \tag{12}$$

Further insight into this nonlinearity can be obtained by considering the opposite limit $(\nu_s/\omega)^{1/2} \ll \phi_1/\phi_0 \ll 1$. In this limit, electrons diffuse much less than a distance $v_1 = (\phi_1/2\phi_0)v_0$ in velocity space during a period $2\pi/\omega$ of the wave. Let the loss cone boundary oscillate as $v(t) = v_0 + |v_1|\cos(\omega t)$. An approximate zero of $f(v)$ exists at $v = v_0 - |v_1|$ because electrons do not have time to diffuse very far between the times when the wave forces $f(v_0 - |v_1|)$ to be zero. All of the electrons are lost from the well in bursts

that occur when $v = v_0|v_1|$, which happens when $\cos(\omega t) = -1$, or $\omega t = \pi, 3\pi, 5\pi, \ldots$. In the nonlinear limit, the number of trapped electrons $n(t)$ as a function of time resembles a sawtooth, with gradual increases interrupted by sharp drops whenever $\cos(\omega t) = -1$.

A related nonlinearity occurs when large angle collisions dominate over small-angle collisions. Figure 1 shows that the unperturbed distribution function $f_0(v)$ changes rapidly on a small scale in this limit ($\alpha \gg 1$). By the same reasoning that led to Eq. (12), we conclude that to be in the linear regime when $\nu_L \gg \nu_s$, we require that $\phi_1/\phi_0 \ll (\nu_s/\nu_L)^{1/2}$.

The linear response has an interesting property in the limit where large-angle scattering dominates ($\nu_L \gg \nu_s$): the response actually depends on small-angle collisions, even though $R(\omega)$ does not formally depend on ν_s in this limit. To understand this, note that the unperturbed distribution function near the loss boundary in this limit is

$$f_0(v) = f^* \left[1 - \exp\left(- \sqrt{\frac{\nu_L}{\nu_s}} \frac{\Delta v}{V_0} \right) \right], \tag{13}$$

where $\Delta v = v_0 - v$, and $f^* = bn_0/2v_0$ is the plateau in the unperturbed distribution function shown in Fig. 1 for $\alpha = 18$. When large-angle collisions dominate, there is a sudden drop of $f_0(v)$ at the loss boundary. The sharpness of this drop depends on diffusion (via ν_s). The response R is proportional to the product of $\partial f_0/\partial v$ times the skin depth of f_1 depend on ν_s, but the dependence cancels when we take the product, so that $R(\omega)$ is independent of ν_s in the limit $\nu_L \gg \nu_s$.

The mechanism for the linear response when large-angle collisions dominate is as follows: Large-angle collisions cause f_0 to be large near the loss point v_0, where f_0 drops from a plateau region f^* to zero within a short distance determined by diffusion. As the loss point fluctuates around v_0, the disturbance in $f(v)$ penetrates by a skin depth, also determined by diffusion. However, the resulting fluctuations in the trapped number $n_0 + n_1 e^{i\omega t}$ have no explicit dependence on the diffusion coefficient. Thus the effect of large-angle scattering in this frequency regime is to distort velocity space so that the response is really due to small-angle collisions.

III. PHYSICALLY REALISTIC MODEL

The ideas developed in Sec. II can be applied to a more realistic three-dimensional model. The approximate equations for the response $R(\omega)$ stated in Eq. (9) are generally found to be valid, although there are some exceptions. The frequencies (ν_s, ν_L, ν_c) all retain their essential meaning (diffusion, large-angle scattering, and confinement, respectively). We define ν_s as follows. Consider an electron with velocity v_0 near the loss boundary. During a small time t, it will diffuse a distance $v_0 (\nu_s t)^{1/2}$ toward or away from the loss boundary. As in Eq. (3), we obtain ν_s from the diffusion coefficient at the loss boundary. On the other hand, ν_c is determined by a weighted average of the diffusion coefficient over all of velocity space. In contrast to the one-dimensional model, we cannot always assume $\nu_s \approx \nu_c$ when small-angle collisions dominate. The bounce-averaged electron distribution function obeys

$$\frac{\partial f}{\partial t} = \frac{1}{2} \nabla \mathbf{D} \nabla f - \nabla P f + \int d^3\mathbf{v} [f(\mathbf{v}') g(\mathbf{v}, \mathbf{v}') - f(\mathbf{v}) g(\mathbf{v}', \mathbf{v})] + S(\mathbf{v}). \tag{14}$$

The first two terms in Eq. (14) represent the Fokker–Planck equation,[18] where $\mathbf{D}$ is a dyadic $\nabla \mathbf{D} \nabla f_1 = (\partial/\partial v_i) D_{ij} (\partial/\partial v_j) f_1$, and P is a drag term. The integrals can represent elastic or inelastic large-angle collisions, and the source $S(v)$ need not be at zero velocity.

The loss boundary is a two-dimensional surface, $\phi(\mathbf{v}) = \phi_0 + \phi_1 \exp(i\omega t)$, where $\phi(\mathbf{v})$ is given by a hyperboloid,

$$\phi = \tfrac{1}{2}[v_z^2 - (\mu - 1) v_\rho^2], \tag{15}$$

where v_z and v_ρ are the components of velocity parallel and perpendicular to the magnetic field, respectively, and μ is the mirror ratio. When the confining potential $\phi_0 + \phi_1 \exp(i\omega t)$ shifts, the surface of the loss boundary moves in the direction $\mathbf{u} = \nabla f/|\nabla f|$. Assuming spherical symmetry in velocity space, Eq. (15) becomes $\phi = v^2/2$, so that $\mathbf{u}$ points radially, and ν_s represents an energy diffusion frequency in this approximation.[15]

The problem simplifies greatly in the high-frequency limit $\omega \gg \nu_c$ because the term $\partial f/\partial t$ on the left in Eq. (14) becomes very large. The only term on the right that can be very large is the one containing $\mathbf{D}$, which is large because f_1 has a very large gradient. This allows us to simplify the dyadic term to the scalar term $D\, d^2 f_1/dv^2$, where the scalar $2D$ equals $\mathbf{uDu}$, and the derivative of f is in the $\mathbf{u}$ direction. As in Eq. (11), f_1 is localized to the proximity of the loss surface, decaying exponentially away from the loss surface with the skip depth $(D/i\omega)^{1/2}$. The integral for the perturbed density $n_1 = \int f_1 d^3\mathbf{v}$ can be immediately integrated in the direction perpendicular to the loss boundary, resulting in an integral over the surface of the loss boundary:

$$n_1 = \frac{\phi_1}{\sqrt{i\omega}} \int d^2\mathbf{v} \frac{|\nabla f_0|}{|\nabla \phi|} \sqrt{D}. \tag{16}$$

This equation is valid at high frequency regardless of whether large-angle or small-angle collisions dominate.

The inverse lifetime in the case where small-angle scattering dominates can be found by considering the diffusion of electrons through phase-space $\mathbf{D} \nabla f_0$. Upon integration over the loss boundary, we obtain the inverse confinement time when diffusion dominates the loss process:

$$\nu_c = \frac{1}{n_0} \int d^2\mathbf{v} |\nabla f_0| D. \tag{17}$$

If we assume a spherically symmetric velocity space (i.e., electrostatic confinement), we obtain from (16) and (17)

$$R(\omega) = \tfrac{1}{2} \sqrt{\nu_c^2/i\omega\nu_s}. \tag{18}$$

This response was obtained by Volosov and Bekhtenev,[15] and can be somewhat smaller than the simple estimate $R \sim (\nu_c/i\omega)^{1/2}$ states in Eq. (9b). [The assumptions stated

at the end of this section yield $R = 0.3A^{-1/4}(\nu_c/i\omega)^{1/2}$, where A is the ionic atomic mass.]

If large-angle collisions dominate the electron loss process, there are usually regions on the loss boundary where f_0 drops abruptly to zero from a plateau value $f^*(v)$ as explained in Sec. I and shown in Fig. 1 for $\alpha = 18$. At high frequency ($\omega \gg \nu_c$), f_1 does not penetrate far into the loss boundary. We can deduce ∇f_0 and f_1 at the loss boundary as in the one-dimensional treatment [see Eqs. (11) and (13)]. Thus small-angle collisions determine the skin depth of both f_0 and f_1, but the response is independent of ν_s, and we obtain for the limit $\omega \gg \nu_c$, $\nu_L \gg \nu_s$

$$n_1 = \frac{\phi_1}{\sqrt{i\omega}} \int d^2\mathbf{v} \frac{f^* \sqrt{\nu_L}}{|\nabla \phi|} . \tag{19}$$

It is often possible to estimate $f^*(\mathbf{v})$ to sufficient accuracy, use $|\nabla f| \sim |\mathbf{v}|$, and make reasonable estimates of R in this regime. The scaling $f^* \sim v_0/V^3$ over an area V^2 on the loss boundary recovers Eq. (9b). The dependence on b shown in Table I for the high-frequency, large-angle collision regime can also be recovered as follows. Suppose electrons are injected anywhere in the trapped region. Let them remain there until they are scattered with a probability b into a region of volume V^3, and a probability $1 - b$ of escaping. Let the electrons in the region of volume V^3 have a probability b of remaining in that same region after each collision, and a probability $1 - b$ of escaping. Probability theory says that $f^* = bn_0/V^3$. If the region of volume V^3 intercepts the loss surface over an area of V^2, and we take $|\nabla f| = V$, then the response is exactly the same as shown in Table I for the high-frequency, large-angle collision regime $\omega \gg \nu_L \gg \nu_s$.

Equation (19) can be violated if large-angle scattering cannot bring electrons to the boundary of the loss cone, so that the plateau $f_0(v) = f^*$ is not formed. In Fig. 4, a personal computer was used to obtain equilibrium distribution functions, assuming two dimensions, uniform scalar D, and inelastic scattering. In Fig. 4(a), a plateau does form as large-angle scattering dominates and particles are injected in a region of phase space where they can scatter to the loss boundary. However, when the source is at the origin, large-angle elastic collisions cannot scatter electrons to the loss boundary. Thus the plateau is absent in Fig. 4(c), and large-angle scattering makes no contribution to the response and confinement time, even though $\alpha = 200$.

The estimate $R \sim (\nu_c/i\omega)^{1/2}$ can be verified for the four cases of Fig. 4 by numerically integrating Eq. (16), on the dark line which served as the loss boundary. The response was $R = C(\nu_c/i\omega)^{1/2}$, where $C = 0.11$, 0.29, 0.48, and 0.45

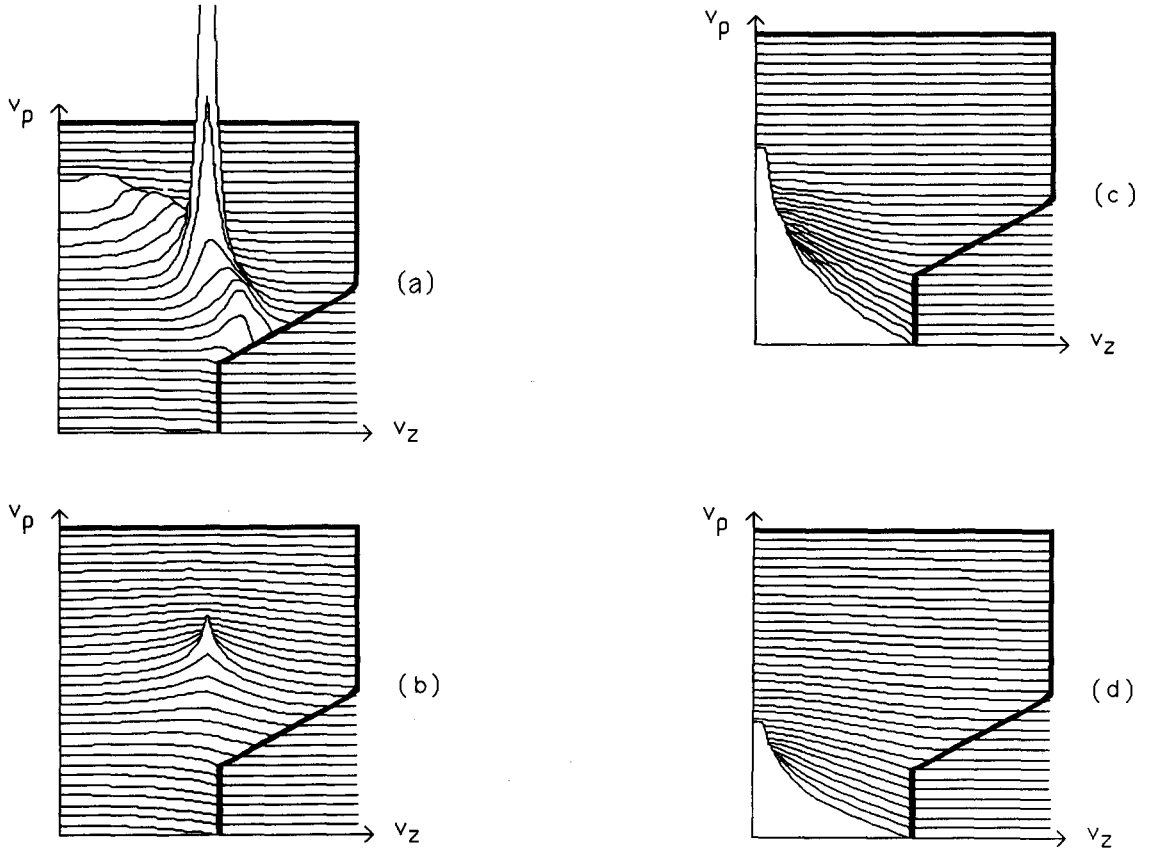

FIG. 4. Distribution functions for a uniform diffusion coefficient in two dimensions with elastic scattering. The dark solid line in the lower right corner is the loss boundary, which corresponds to a mirror ratio of 2. Large-angle scattering should dominate in (a) and (c) because $\alpha = 200$. Small-angle scattering dominates in (b) and (d) where $\alpha = 0.2$. The plateau $f(v) = f^*$ forms in (a) as electrons are scattered from the peak to the loss boundary, but the plateau does not form in (c) because scattering to the loss boundary from $v = 0$ is impossible.

for cases (a) through (d), respectively. The anomalously low value for (a) may be due to the grid being too large to calculate the derivative of f_0. Application of Eq. (19) to case (a) yields $C \approx 0.5$.

Another exception to the estimate $R \sim (\nu_c/i\omega)^{1/2}$ occurs when electrons have high energy. These electrons are confined magnetically, so that confinement is not affected by changes in potential. This is reflected by the large term $|\nabla f| \sim v$ in the denominator of Eqs. (16) and (19).

A more subtle violation of the estimate $R \sim (\nu_c/i\omega)^{1/2}$ could frustrate efforts to line tie interchange modes. Inspection of Eq. (18) shows that the response depends on the diffusion coefficient at the loss boundary via ν_s. If for some reason D is very large in a small region very close to the loss boundary, it will have almost no influence on the electron loss rate ν_c. (This statement seems to contradict Eq. (17), but note that ∇f_0 will get small as D gets large.) Electrons near the loss boundary of velocity space have orbits that take them close to the end wall, where they might experience anomalous turbulence that the bulk of the electrons avoid. Anomalous scattering that is restricted to the extreme edge of velocity space will affect neither the confinement time nor the bulk of the distribution function. Optimistic low estimates of ν_s may be incorrect, even though there is no other indication the classical Fokker–Planck theory inadequately describes velocity space.

IV. APPLICATION TO INTERCHANGE MODES

We define a response $R_f(\omega)$ due to flute modes that describes charge that enters a flux tube by crossing magnetic field lines. We first consider a model for the interchange mode that is equivalent to the ideal magnetohydrodynamic (MHD) approximation at low beta (plasma/magnetic pressure ratio). For an axisymmetric plasma with mirror ratio μ between 2 and 9, the response R_f due to flute modes is[10]

$$R_f = \frac{\phi_0}{T_i}\frac{m^2a^2}{r^2}\left(1+\frac{\gamma^2}{\omega^2}\right),$$

$$\gamma \approx 2\ln(\mu)\left[(T_i+T_e)/2T_i\right]\nu_{Ti}, \qquad (20)$$

where m is the azimuthal mode number, a is the ion Larmor radius, r is the plasma radius, and ν_{Ti} is the ion transit frequency across the length of the mirror $\nu_{Ti} = v_i/l$. The effect of "bad" curvature in R_f manifests itself in the term containing the MHD growth rate γ. The dispersion relation for an interchange mode is $R + R_f = 0$, where R is the line-tying response. Following Ref. 10, we make an analogy to an oscillator or LRC circuit, where "Q" defines the degree to which the modes at $\omega = \pm i\gamma$ of Eq. (20) are damped: $Q = R_f(\infty)/R(\gamma)$. If $Q \gg 1$, then line tying has little effect on the curvature driven interchange mode.

If $Q \ll 1$, then Eq. (20) shows that ω must approach zero in order for the responses due to curvature and line tying to cancel. The growth rate of the interchange mode is reduced to approximately $0.5Q^{2/3}\gamma$ in the limit $Q \ll 1$. This remains valid if we use a more complicated model[7–9] for the interchange mode that considers finite ion Larmor radius and a radial electric field that causes the plasma to rotate with angular frequency ω_E. Inspection of Eq. (4) of Ref. 9 shows that the response due to curvature diverges at $\omega = \omega_E$. (The response of Ref. 9 may be normalized to our definition if we multiply by $-\phi_0/en_0$ and replace ω by $-\omega$.) For a rotating plasma we may Doppler shift the line-tying response to $R(\omega - \omega_E)$. Thus in the limit $Q \ll 1$, the more complete response yields the same growth rate $0.5Q^{2/3}\gamma$, with the real part of the frequency being very close to ω_E. Also, the centrifugal force contributes to the growth rate, and line tying inhibits finite Larmor radius stabilization, as was first noted in Ref. 19 using the Kunkel–Guillory model.

We can estimate Q by making reasonable assumptions about the plasma parameters, and by assuming that both ν_s and ν_c can be estimated from the Spitzer collision frequencies.[17,18] Since ν_s describes electrons far above the thermal energy, we follow Ref. 15 and we use $\nu_s \approx (T/\phi)^{5/2}\nu_{ee}$, where $\nu_{ee} = 4\times10^{-6}nT^{-3/2}\ln\Lambda$ is the thermal electron diffusion time,[16] with the density n measured in cm^{-3}, electron temperature T in eV, and the Coulomb logarithm $\ln\Lambda \sim 15$. For the inverse confinement time, we take $\nu_c \approx \nu_{ii} = (m_e/m_i)^{1/2}\nu_{ee}$, which is the time for ions to scatter 90 deg. We also set $T_e = T_i$, $\phi_0/T = 3$, $\gamma = 4\nu_T$, and mirror length $l = 200$ cm.

When ν_{Ti}/ν_c is large, it is convenient to define $K = \nu_{Ti}/\nu_c = 5\times10^9T^2n^{-1}$ as the average number of times an ion transits the mirror before exiting. If we define $\rho = r/a$ as the plasma radius normalized on the Larmor radius, we obtain a simple expression: $Q \approx 20m^2A^{1/4}K^{1/2}\rho^{-2}$, where A is the ionic atomic mass, and we require $K \gg 1$ since the electrons and ions have comparable mean-free paths. By contrast, if the Kunkel–Guillory model [Eq. (10)] is incorrectly applied to the collisionless regime, we would obtain a value of Q that is larger by an amount $0.6K^{1/2}$ for hydrogen (or $2K^{1/2}$ for barium).

Figure 5 shows a map[17] of plasma density and temperature. More line tying (low Q) occurs in the upper left, and

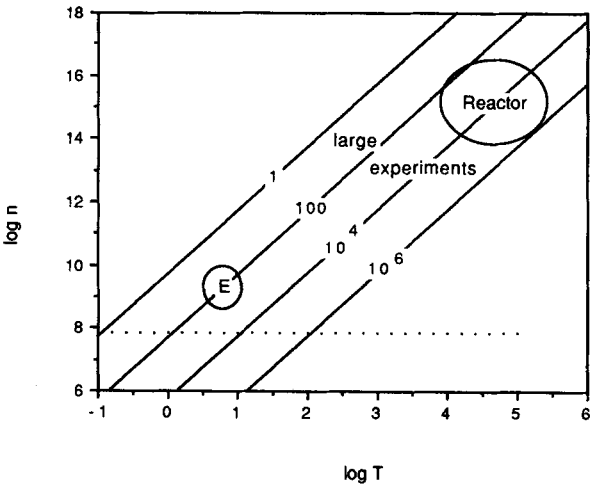

FIG. 5. A map of density versus temperature. The diagonal straight lines are contours of $K = 1$, 100, 10^4, and 10^6, where $K = \nu_{Ti}/\nu_{ii}$ is a measure of the number of bounces an ion in a mirror of length 200 cm will experience before being scattered out of the mirror. If the normalized radius $r/a = 40$, then the contours of K are contours of $Q = 0.02$, 0.2, 2, and 20. If $r/a = 4$, then the lines are contours of $Q = 2$, 20, 200, and 2000. All values are for lithium, and the values of Q assume a confinement time of ν_{ii}.

less line tying in the lower right part of this map. The diagonal straight lines are contours of $K = 1$, 100, 10^4, and 10^6 for a mirror of length 200 cm. For example, a fusion plasma with normalized radius $\rho \sim 40$ has $K \sim 10^5$ bounces, and therefore $Q \sim 10$ for the $m = 1$ mode. The target parameter regime for the experiment at Dickinson College is marked with a letter "E" in the figure. For a small experiment with $\rho \sim 4$, we would obtain $Q \sim 20$ if we really could confine the ions of $K = 100$ bounces. In reality, the confinement in the experiment is not expected to exceed ten bounces due to collisions with neutral particles, so that we are striving to achieve $Q \sim 3$. Note that the Kunkel–Guillory model yields $Q \sim 3000$ for a fusion reactor, and $Q \sim 1$ for the Dickinson experiment.

The horizontal dotted line in Fig. 5 represents an ion plasma frequency $4\pi ne^2/m_i$ that is ten times the ion cyclotron frequency eB/m_ic^2 at $B = 1$ kG, for a lithium plasma. The plasma density must exceed this limit in order to obtain quasineutrality for the flute mode,[7-9] which means that the perturbed ion and electron densities are equal, and requires that the ion plasma frequency $4\pi ne^2/m_i$ far exceed the ion cyclotron frequency eB/m_ic^2.

Although line tying has been investigated[20] with a hot, dense plasma on Phaedrus[21] at the University of Wisconsin, the relevant equations for interchange modes allow one to mimic a hot, dense plasma using a cold, tenuous plasma.[7-9] (The cold, tenuous plasma fails to properly scale the effect of high "beta," where beta is the ratio of plasma pressure to magnetic pressure.[10]) Typical temperatures are 0.3 to 3 eV, with densities of 10^9 to 10^{10} cm^{-3}, and a magnetic field of the order of a kilogauss. Such experiments have been carried out at the University of California at Berkeley[6] and at Irvine.[5,9,10,20,22]

The experiment at Dickinson College will operate at a lower density than is customary for "cold" plasma experiments in order to reduce the collisionality of the plasma. The plasma will be injected radially,[23] not axially as is usually done. This will ensure that the plasma is mirror trapped, and will accommodate diagnostics at the end walls.[16] The low plasma density might lead to a situation where large-angle scattering of neutrals is the dominant loss mechanism for electrons. However, as shown at the end of Sec. II, the linear response is due to small-angle Coulomb collisions.

V. CONCLUSION

We have considered the response of trapped electron number to fluctuating potential, focusing on time scales where the potential fluctuates on an ion transit time scale. Both large- and small-angle scattering yield almost identical responses. Furthermore, the physical mechanism for the response due to large-angle scattering is actually small-angle scattering at the loss boundary. We now have two different responses. The original Kunkel–Guillory model remains valid when the electron mean-free path is smaller than the machine length ($K \ll 1$), while a new collisionless response applies when $K \gg 1$. The collisionless response can become nonlinear at low amplitudes.

When the collisionless model is applied to interchange modes in a fusion reactor, it predicts a degree of line tying that is about 300 times larger than had been predicted using the collisional model. A mirror in the fusion regime with relatively high density and low temperature might be significantly influenced by line tying for the $m = 1$ mode. However, any attempt to design a line-tied axisymmetric mirror fusion reactor will probably have to use blanket and/or feedback stabilization, because higher-order modes are much less influenced by line tying, and because line tying for the $m = 1$ mode on a fusion reactor could not reduce the growth rate more than an order of magnitude below the ideal MHD growth rate of $4\nu_{Ti}$ for an axisymmetric mirror. However, this new analysis does indicate that the blanket of a blanket-stabilized fusion reactor need not differ too greatly from the core plasma.

Several conclusions can be drawn concerning parameters of a small plasma device designed to study line tying in fusion research. First, the device must confine ions for several bounces, so that we are in the collisionless regime. Second, we need not concern ourselves with whether scattering with neutrals contributes to particle losses and line tying because large-angle and small-angle scattering yield similar forms of line tying. Finally, an experiment to test this theory on a small device cannot focus on an estimate of $|R(\omega)|$, but must instead focus on the different ω dependencies predicted by the collisional Kunkel–Guillory model, and the collisionless model proposed by Volosov and Bekhtenev.

Future work will continue in three directions. A low-density mirror experiment is being constructed that should put line tying in the collisionless regime. Second, the numerical studies of blanket stabilization by Segal[4,5] need to be extended to the case where the blanket is collisionless ($K > 1$ in Fig. 5). Finally, the consequences of the low-amplitude nonlinearity of the response need to be understood.

[1] W. K. Kunkel and J. Guillory, in *Proceedings of the 7th International Conference on Phenomena in Ionized Gases*, edited by B. Perovic and D. Tosic (Gradevinska Knjiga, Beograd, Yugoslavia, 1965), Vol. 2, p. 702.
[2] R. F. Post, R. E. Ellis, F. C. Ford, and M. N. Rosenbluth, Phys. Rev. Lett. **11**, 166 (1960).
[3] B. Lehnert, Phys. Fluids **9**, 1367 (1966).
[4] D. Segal, M. Wickham, and N. Rynn, Phys. Fluids **25**, 1485 (1982).
[5] D. Segal, Phys. Fluids **26**, 2565 (1983).
[6] M. A. Lieberman and S. K. Wong, Plasma Phys. **19**, 745 (1977).
[7] M. N. Rosenbluth and A. Simon, Phys. Fluids **8**, 1300 (1965).
[8] M. N. Rosenbluth, N. A. Krall, and N. Rostoker, Nucl. Fusion Suppl. Part I, 143 (1962).
[9] M. Wickham and G. Vandegrift, Phys. Fluids **25**, 52 (1982).
[10] G. Vandegrift and T. Good, Phys. Fluids **29**, 550 (1986).
[11] G. D. Hobbs and J. A. Wesson, Plasma Phys. **9**, 85 (1967).
[12] G. D. Porter, Nucl. Fusion **22**, 1279 (1982).
[13] R. Prater, Phys. Fluids **17**, 193 (1974).
[14] A. A. Bekhtenev and V. I. Volosov, Zh. Tech. Fiz. **47**, 1450 (1977) [Sov. Phys. Tech. Phys. **22**, 834 (1977)].
[15] A. A. Bekhtenev, G. Vandegrift, and V. I. Volosov, Fiz. Plasmy **14**, 292 (1988) [Sov. J. Plasma Phys. **14**, 168 (1988)].
[16] G. Vandegrift, submitted to Rev. Sci. Instrum.
[17] See National Technical Information Service Document No. ADA 041545/[NRL Memo. Report No. 3332, "NRL Plasma Formulary," edited by D. Book (1980)]. Copies may be ordered from the National Technical Information Service, Springfield, Virginia 22161. The price is $18.95 plus a $3.00 handling fee. All orders must be prepaid.

[18] S. Ichimaru, *Basic Principles of Plasma Physics* (Benjamin, Reading, MA, 1973).
[19] J. C. Riorden and C. W. Hartman, Phys. Fluids **20**, 1378 (1977).
[20] J. Pew, R. A. Bruin, T. N. Good, N. Hershkowitz, B. Nelson, and G. Vandegrift, Bull. Am. Phys. Soc. **28**, 1203 (1983).
[21] J. J. Browning, R. Majeski, T. Intrator, and S. Meassick, Phys. Fluids **31**, 714 (1988).
[22] G. Vandegrift and T. Good, Bull. Am. Phys. Soc. **28**, 1048 (1983).
[23] Y. Kiwamoto, Rev. Sci. Instrum. **51**, 285 (1980).